Study of Conducting Properties of Chemically Synthesized Polyaniline/crystalline Silica Composites

Tehseen Riaz,[1] Farah Kanwal,[2] Saadat Anwar Siddiqi,[3] Nafisa Gull,[2,4] Tahir Jamil,[4] Akbar Ali,[5] Aisha Batool,[1,5] ShahNawaz Phulpoto,[6] and Khalid H. Thebo[7*]

[1] *Centre of Excellence in Solid State Physics, University of the Punjab, New Campus Lahore-54590, Pakistan*
[2] *Institute of Chemistry, University of the Punjab, New Campus Lahore-54590, Pakistan*
[3] *Interdisciplinary Research Centre in Biomedical Materials, COMSATS Institute of Information Technology, Defense Road, Off Raiwind Road, Lahore-54500, Pakistan*
[4] *Institute of Chemical Engineering & Technology, University of the Punjab, New Campus Lahore-54590, Pakistan*
[5] *National Center for Nanoscience and Technology, University of Chinese Academy of Sciences, Beijing-100190, China.*
[6] *State Key Lab of Chemical Resource Engineering, Beijing University of Chemical Technology, Beijing, China*
[7] *School of Chemistry and Materials Science, University of Manchester UK, Oxford Road, M13 9PL Manchester UK.[*]*

Abstract— Conducting polyaniline (PANI) and polyaniline/SiO$_2$ composites with significantly high conductivity were synthesized via facile oxidative polymerization method using potassium dichromate (K$_2$Cr$_2$O$_7$) as oxidizing agent at 0°C. PANI/SiO$_2$ composites with different weight ratios of crystalline silica were prepared in order to evaluate their electrical conductivity. Their structural and thermal properties were also investigated by using X-ray diffraction (XRD) and thermo gravimetric analysis (TGA) techniques. The insertion of silica into PANI up to specific weight percentages gives a 10 fold increase in conductivity. Microstructural analysis by scanning electron microscopy (SEM) reveals that a specific type of inter-connecting morphology is essential for obtaining an optimal electrical conductivity. Such a condition is attained with a specific amount of silica distribution in the composite. SEM study showed that polyaniline/SiO$_2$ composites maintain a conducting micro-structural network up to 20wt-% silica inclusion by giving a maximum electrical conductivity of 40S.cm^{-1} due to better de-localisation of electrons and improvement of the inter-particle processes for the charge transport.

Key words: polyaniline, polymerization, composite, FTIR, SEM, TGA, Conductivity.

————————————— ◆ —————————————

1 INTRODUCTION

Intrinsically conducting polymers (ICPs) are organic polymers with an alternating single and double bond π framework between the atoms that possess electrical, electronic and optical properties of a semiconductor or metal while retaining the properties associated with conventional polymers.[1, 2] The unique properties of conducting polymers have led to a variety of applications.[3, 4] However, many of its potential applications are not completely explored due to their inferior thermal and mechanical properties.[5] ICP Composites containing inorganic fillers of special properties improve such properties of conducting polymers. Polyaniline (PANI) is domineering member among the em-inent class of ICPs in materials science owing to its good environmental stability, ease of synthesis and good conductivity and process ability.[6] Its emeraldine salt form has been studied to great extent being most conducting one.[5] Among the numerous PANI/inorganic composites, PANI/silica composites received much attention in recent years and most commonly reported in literature. Within the past decades, many reports have been published on the polyaniline/silica composite systems describing the effect of combining PANI and various forms of silica on conductive properties of resulting composites.

In the design of polyaniline/silica composites, a

number of composites with silica sol[7], fumed silica[8], nano silica[9], porous and spherical nano-SiO_2[10-12],mesoporous and colloidal silica particles[13-18] have been developed and characterized for their electrical conductivity. In addition, the conductive properties of polyaniline/silica hybrid composites[19], polyaniline /silica nancomposites (NPs)[20] and PANI/SiO_2 composite films[21, 22] have also been investigated. The conductivity of these composites was found in the range 10^{-11} to 25 S.cm[-17-10, 13-22] and was found to be either improved or reduced after the addition of silica. In some reports composites showed percolation behavior with percolation threshold obtained at the specific weight ratios of silica to PANI.[8, 22] Although all above studies have reported electrical conductivity of PANI/silica composites, we, in this context, report polyaniline/crystalline silica (quartz) composites with maximum conductivity of 40 S.cm^{-1} at percolation limit which has not been achieved yet for PANI/silica composites. Influence of the presence of silica insulating framework on electrical conductivity of PANI is also discussed. Firstly we synthesized emeraldine salt of polyaniline using chemical polymerization and compare conductivity of resultant polyaniline with that our group has previously achieved.[23] Secondly, polyaniline composites with crystalline silica are chemically synthesized in good yield and high conductivity. Different percentages of silica (5-40wt-%) were added into Polyaniline matrix to allow silica contribution to electrical conductivity of composites.

2. Experimental procedure
2.1. Materials

Aniline monomer from Riedel-deHaën was purified by distillation process prior to use and stored in Nitrogen environment at 4°C. Potassium dichromate ($K_2Cr_2O_7$) from Riedel-deHaën was used as oxidant in aqueous medium. Hydrochloric acid (HCl) from Analar was used as dopant. SiO_2 (reagent grade) from Fluka was used in this research work. All solutions were prepared in deionized water.

2.2. Synthesis of Polyaniline

HCl doped polyaniline has been previously synthesized by our group.[23] In the present work, we synthesized polyaniline by using same reactants as previously[23] but with different molar ratios. A 0.2:0.7 molar ratio of Aniline: $K_2Cr_2O_7$ and 3.5: 0.2 molar ratio of HCl: Aniline is used in present experiment. 4ml of distilled aniline was mixed with 20 ml of HCl solution and cooled to 0°C. 25ml of $K_2Cr_2O_7$ solution was added drop wise into above solution in 1 hour under constant stirring of 24h and nitrogen flow at 0°C. The dark green solution was allowed to stay at 0°C to complete polymerisation. The precipitate of PANI were collected by filtration and washed with HCl solution, acetone and

deionized water to remove unreacted monomers, impurities and by-products and were dried at 50°C in oven for 48 hours. Table 1 presents the reactant molar ratios of previous and present experiments namely E1 and E2 respectively. (Table 1)

After preparing pure polyaniline, its DC conductivity was measured by pressing dried precipitates into cylindrical discs. As given in Table 1, conductivity of PANI obtained from E2 is higher than that of E1; therefore molar ratios of E2 were selected for preparing polyaniline composites with silica.

2.3. Synthesis of Polyaniline/SiO_2 Composites

In experiment two (E2), after complete dropping of $K_2Cr_2O_7$ solution into aniline & HCl mixture, different percentages of SiO_2 (5, 10, 20, 30 and 40wt-% of PANI yield) were added to reaction mixture and named as PANI/SiO_2-5, PANI/SiO_2-10, PANI/SiO_2-20, PANI/SiO_2-30 and PANI/SiO_2-40. The reaction mixture was stirred for 24 h at 0°C to disperse SiO_2 particles homogeneously. The precipitates of all composites were collected, washed and dried using similar protocol described in section 2.2.

2.4. Instrumentation

Fourier Transform Infrared (FTIR) spectra of polyaniline and PANI/SiO_2 composites were obtained at room temperature using Perkin Elmer RXI FTIR spectrometer at resolution of 4.0 cm^{-1} over 70 scans having ATR accessory in the range of 650-4000 cm^{-1}. Samples were dispersed in Potassium Bromide (KBr) and compressed into pellets for taking spectra. X-ray powder diffraction analysis was used to determine the phases and crystallite sizes of samples. Measurements of the samples were taken on Rikgaku D-Max/IIA diffractometer using CuK_α (λ = 1.54Å). Ni was used as a filter to suppress the K_β component. The range of diffraction angle was fixed from 2θ = 5-80° with step width of 0.05. The thermal stability of pure PANI and PANI-SiO_2 composites were examined by SDT Q600. The samples were heated from 20 to 800 °C under an air atmosphere flow condition with a flow rate of 20 °C/min. An aluminum pan was used as a reference. The calorimeter cell was flushed with 100 mL min^{-1} of nitrogen. JSM-6480 scanning electron microscope was used for microstructure analysis. SEM was operated at secondary electron imaging mode. All images were obtained at an accelerating voltage of 15 KV. DC conductivity was measured by standard four probe technique. Each sample powder was pressed into pellet under pressure of 6 tons by using Apex hydraulic press. A digital Multimeter (M 2007) was used to measure applied voltage across the circuit and corresponding current values were measured from professional Pro's Kit Multimeter. Conductivity was measured as reported previously.[1, 2]

*Corresponding author, Tel: +86-15542152720
e-mail address: khalidthebo@yahoo.com

3. Results and Discussion

3.1 Fourier transforms infrared spectroscopy

The FTIR spectra of SiO_2, PANI and $PANI/SiO_2$ composites are shown in Figure 1. The spectra reveal that the composites contain all main characteristics bands of polyaniline [24, 25] and silica.[26] Figure 1 gives the FTIR spectrum of pure PANI. The absorption band at 3435 cm^{-1} corresponds to N-H stretching of PANI. The band at 2991 cm^{-1} is assigned to aromatic C-H stretching. The peaks at 1582 cm^{-1} and 1453 cm^{-1} are attributed to C=N and C=C stretching modes for quinoid and benzenoid rings. The band at 1288 cm^{-1} corresponds to C-N stretching vibrations originating from bipolaron structure and confirms conducting emeraldine salt form of PANI[27]. The peak at 1153 cm^{-1} is the characteristic peak of PANI conductivity and is considered to be the measure of degree of charge delocalization of on polymer backbone[28]. The band at 1026 cm^{-1} is assigned to C-H in-plane bending vibrations.
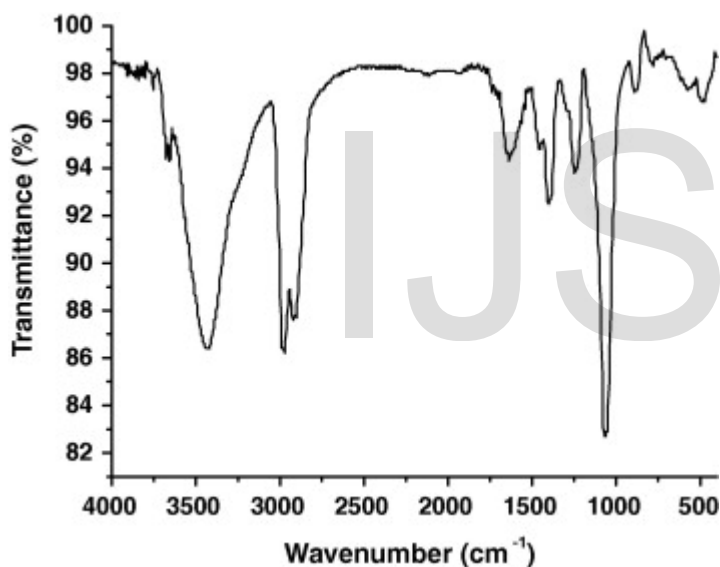
(113) and (220) planes of SiO_2 crystals respectively. These peaks were consistent with the standard peaks of alpha quartz (JCPDS card No 5-0494). The other peaks at 28.95º, 22.68º, 46.10º, 24.13° and 73.68º in pattern are due to impurities present in SiO_2. In XRD patterns of $PANI/SiO_2$ composites crystalline phases of SiO_2 appear superimposing on the amorphous pattern of PANI. The four major peaks at 2θ = 26.69°, 20.81°, 50.33° and 60.13° in all the samples containing SiO_2 correspond to (101), (100), (112) and (211) planes of SiO_2 crystals. In $PANI/SiO_2$-5 and $PANI/SiO_2$-10, the above peaks are weak and indicate semi crystalline nature of these composites as compared to pure PANI. Increase in SiO_2 content from 20-40% enhanced the crystalline phase of composites with appearance of some other peaks at 39.59°, 36.75°, 2.70°, 55.30°, 68.20°,75.91°, 64.21° and 77.80° and all peaks were matched with theJCPDS card No 5-0494. Intensities of all peaks also increase gradually with an increase of SiO_2 percentage in the composites.
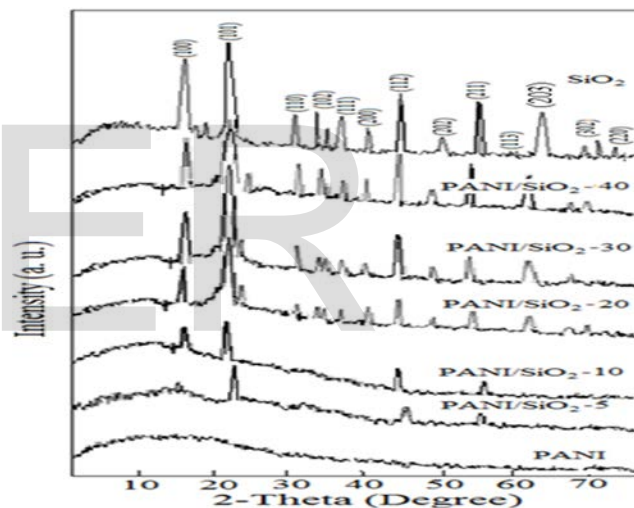

Figure 1. The FTIR spectrum of $PANI/SiO_2$ composites

Figure 2. XRD pattern of pure Polyaniline, SiO_2 and their composites with different ratios

3.2 X- ray diffraction analysis

Figure 2 showed the XRD pattern of pure Polyaniline, SiO_2 and their composites. Pure PANI showed a broad hump near 2θ = 20° due to the scattering of X-rays from polyaniline chains at interplaner spacing[29] and indicates the amorphous structure of PANI. The XRD pattern of SiO_2 shows that SiO_2 is purely crystalline. The observed peaks at 2θ = 26.83°, 21.04°, 50.35°, 60.21°, 68.14° 39.59°, 36.75°, 42.70°, 55.30°, 40.50°, 75.91°, 64.21° and 77.80° correspond to the diffraction from (101), (100), (112), (211), (203), (102), (110), (200), (202), (111), (302),

Exp.	Ani (m)	K2Cr2O7 (m)	HCl (m)	[HCl]/ [Ani]	[Ani]/ K2Cr2O7	Reaction condition (C)	Conductivity S/cm
E-1	0.2	0.1	2	10	2	0	3.7
E-2	0.2	0.7	3.5	17.5	0.28	0	5

Table 1: Reactants molar ratios and resultant conductivity of two different Experiments (E1 & E2)

3.3. Thermogravimetric Analysis

*Corresponding author, Tel: +86-15542152720
e-mail address: khalidthebo@yahoo.com

The thermal behavior of PANI with different particle loadings was represented in Figure 3. All the samples show three step degradation trend at the temperature ranging from 20℃ to 800℃. Thermogram of pure PANI (curve a) shows an initial weight loss of 20% at the temperatures below 120℃ due to elimination of moisture [30]. The second stage loss from 120℃ to 290℃ is associated with the loss of low molecular weight oligomers [31]. The polymer decomposition step starts at the temperatures higher than 300℃. The weight loss of 56% of pure PANI occurred in the temperature range 290 ℃-800 ℃ is associated with the thermal degradation of organic moieties in PANI unit and the residue remained at 800 ℃ is 44%. SiO_2 shows a total weight loss of 1.4% in one step complete decomposition due to its very high thermal stability. The thermal stability increases sharply with the increase of SiO_2 content (5-40wt. %) in PANI. Among the composites, PANI/SiO_2-40 shows highest thermal stability with 76.6% residue at 800℃. The continuous increase in thermal stability with the increase of particle loading is due to significant barrier effect of SiO_2 which shields the polymer decomposition or may be due to coordination bond interactions between PANI and SiO_2 particles as inferred from FTIR results. Adsorption of polymer chain onto filler particles surface restricts the segmental mobility of polymer units which also improve the thermal stability of composites.
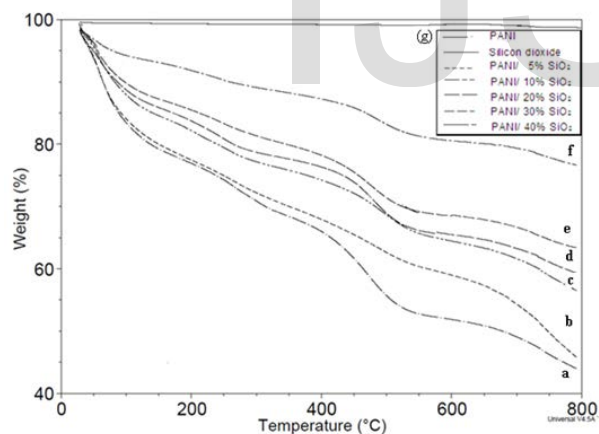

Figure 3. TGA studies i.e. thermal behavior of PANI with different particles.

clusters with weak linkage between PANI chains and has relatively high porosity. The micrographs of composites showed that the silica loading concentration has significantly affected the morphology of PANI after composite formation. The micrograph clearly shows two distinct phases, one relatively dark and the second phase lighter in color. One can associate them with polyaniline and silica. However, the abridging nature of silica particles between the polyaniline matrixes is very obvious in this micrograph.

3.4. Scanning Electron Microscopy

Figure 4 (a-c) presents the morphology of PANI/SiO_2 composite with 0wt-%, 20wt-% and 30 wt-% silica loading examined by SEM. The SEM micrographs of pure polyaniline and composite containing 30wt-% silica loading reveal that pure PANI exists in the form of globular
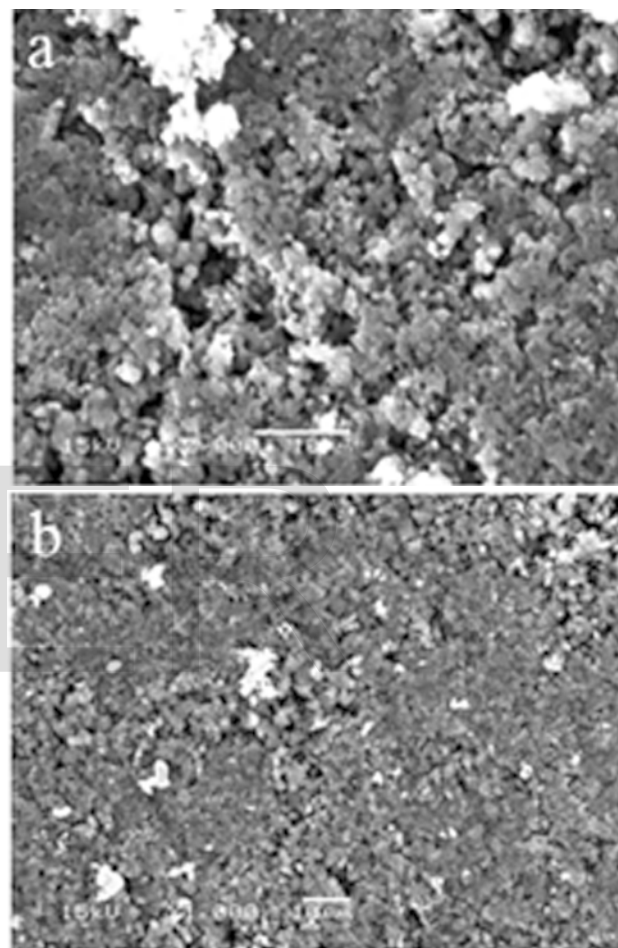
*Corresponding author, Tel: +86-15542152720
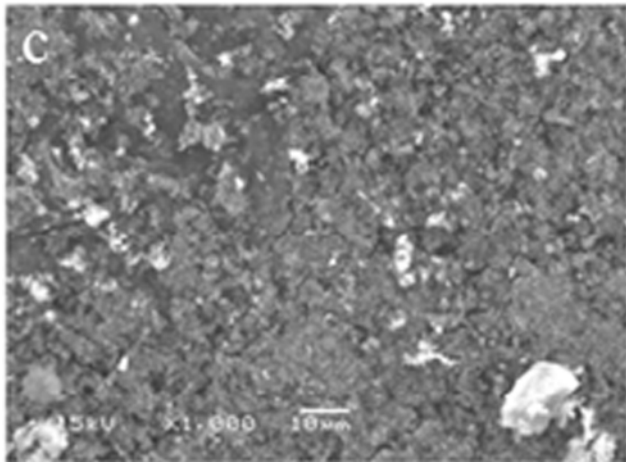e-mail address: khalidthebo@yahoo.com

Figure 4. SEM images of PANI/SiO$_2$ composite with 0wt-%, 20wt-% and 30 wt-% silica loading.
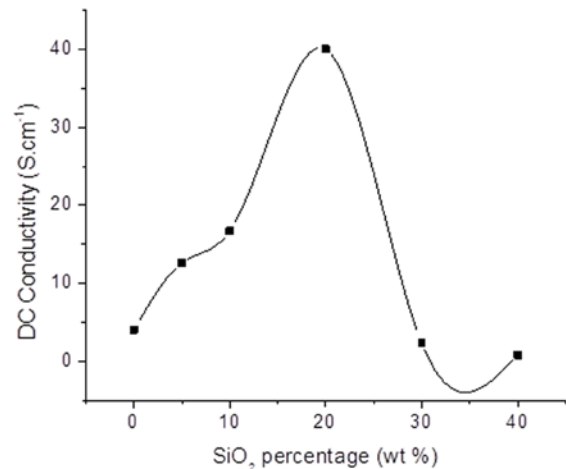

Figure 5. Variation in conductivity of prepared PANI/SiO$_2$ composites with SiO$_2$ content

3.5. Electrical Conductivity
3.5.1. Conductivity of Polyaniline for different Experiments

The difference in conductivity value of pure polyaniline synthesized in E1[23] and E2 (Table-1). It is seen that variation in the molar ratios ([Ani]:[K$_2$Cr$_2$O$_7$] and [HCl]:[Ani]) cause an increase the conductivity of PANI prepared at same temperature and atmospheric conditions. As electrical conduction of PANI depends on doping level, therefore increasing thedopantto aniline ratio (Table 1) by increasing the degree of doping (using 3.5M HCl) may generate more charged species and increase the conductivity of PANI.

3.5.2. Conductivity of PANI/SiO$_2$ Composites

Variation in conductivity of prepared PANI/SiO$_2$ composites with SiO$_2$ content is depicted in Figure 5 and Table-2. Figure 5 indicated that the percolation threshold of PANI/SiO$_2$ system was achieved at 20wt-% of SiO$_2$ content in PANI. The room temperature current-voltage *(I-V)* measurements of PANI and all composites revealed good Ohmic behavior over a wide range of current as given in Figure 6.

The conductivity of present PANI/silica composites obtained at 20wt-% silica (40S.cm^{-1}) is premier value of conductivity among earlier reports on different PANI/silica composites by different groups[7-10, 13-22](as described section 1). All these studies have been focused on achieving conducting composites of polyaniline by introducing different kinds of silica particlesinto organic phase.Recently conductive PANI/SiO$_2$ composite films were found to have improved conductivity after SiO$_2$ addition up to specific weight percent (10wt-% SiO$_2$ in PANI).[21, 22] It was found that composites showed a maximum conductivity of 9.8 S/cm at percolation limit (at 10wt-% SiO$_2$ content).[22]However variations in conductivity values for different SiO$_2$ contents were a bit gradual and maximum conductivity of composites was not much high; here the crystalline silica distribution in polyaniline at 20wt-% loading makes acomposite that potentially offers such a high conductivity (40S.cm^{-1}). Theremarkable aspect of Figure 5is the abrupt variations in the conductivity values of composites before and after percolation limit (20wt-% SiO$_2$). These variations can be explained by morphological features of composites. The composite with particle loading of 20wt-% SiO$_2$ shows a homogeneous dispersion of SiO$_2$ particles in polymer matrix as can be seen in Figure 4. At this loading, the linkage of PANI chains with the help of SiO$_2$particlespromotes strong interactions between PANI molecules and SiO$_2$ particles due to which charge transfer from PANI units to SiO$_2$ particles overcomes the Vander Waals interaction between SiO$_2$ particles and hence impede SiO$_2$ aggregates.[22] Enhanced grain-to-grain linkages at 20wt-% particle loading provide continuous conducting pathways for the movement

*Corresponding author, Tel: +86-15542152720
e-mail address: khalidthebo@yahoo.com

of carriers. In addition to the continuous network due to physical contact among particles, the hoping of electron between two particles separated by few nanometers also enhances the carrier transport. The dramatic increase in the conductivity from 10 to 40 S.cm^{-1} may be attributed to the presence of very efficient conducting network as well as pronounced tunneling mechanism of carriers at 20wt-% silica loading.
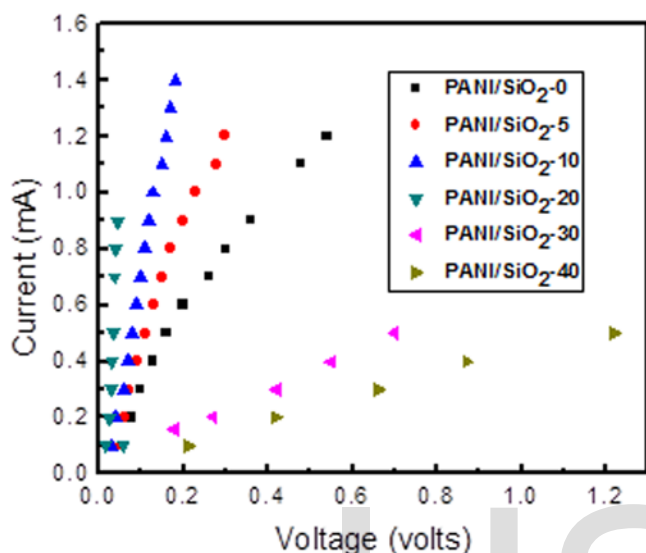

Figure 6. Graphical represenataion of DC conductivities of composites as a function of SiO$_2$ content

Sample Name	Conductivity (S.cm^{-1})
PANI/SiO$_2$-0	4
PANI/SiO$_2$-5	12.6
PANI/SiO$_2$ -10	16.7
PANI/SiO$_2$ -20	40.0
PANI/SiO$_2$ -30	2.3
PANI/SiO$_2$-40	0.8

Table 2: DC conductivities of composites as a function of SiO$_2$ content

The density of SiO$_2$ particles in matrix has increased to a saturation value when SiO$_2$ content was increased to 30wt-%; as a result silica aggregates appear in various regions of PANI matrix (Figure 4c). The sharp decline in conductivity of PANI/SiO$_2$-30 and PANI/SiO$_2$-40 may be due to wrecking of conductive network of PANI and due to aggregation of SiO$_2$ particles which strongly hamper the charge carrier motion through PANI matrix.

4. Conclusions

By introducing silica to polyaniline solution during polymerization, we prepared highly conducting polyaniline/silica composites.Pure polyaniline was prepared by chemical oxidative method and obtained conductivity of polyaniline is compared to conductivity results from our previous work23on polyaniline. It was found that using the following molar ratios: [Aniline]:[K2Cr2O7] = 0.28 and [HCl]:[Aniline] = 17.5in PANI synthesis gives high conductivity of polyaniline, therefore these molar ratios were used to prepare PANI/silica composites with various silica percentages. Thermogravimetric analysis (TGA) demonstrates higher thermal stability of PANI-SiO2 composites with a considerable reduction of weight loss. The measured electrical conductivity of composites was the function of amount of dispersive phase. Percolation was achieved at around 20wt-% silica with conductivity of 40S.cm-1. Conductivity measurements coupled with SEM analysis showed that more than 20wt-% silica loadings greatly weakens the connectivity between the conducting PANI chains and reduce the composites conductivity.

REFERENCES

1. F. Kanwal, S. A. Siddiqi, A. Batool, M. Imran, W. Mushtaq, and T. Jamil, *Synth. Met.*, 2011, **161**(3), 335-339.
2. A. Batool, F. Kanwal, M. Imran, T. Jamil, and S. A. Siddiqi, *Synth. Met.* , 2012, **161**(23), 2753-2758.
3. A. B. Moghaddam, T. Nazari, J. Badraghi, and M. Kazemzad, *Int. J. Electrochem. Sci.* , 2009, **4**, 247-257.
4. M. Gerard, A. Chaubey, and B. Malhotra, *Biosens. Bioelectron.* , 2002, **17**(5), 345-359.
5. W. L. Zhang, Y. D. Liu, and H. J. Choi, *Carbon*, 2012, **50**(1), 290-296.
6. Y.-W. Lin and T.-M. Wu, *Compos. Sci. Technol.* , 2009, **69**(15), 2559-2565.
7. D. J. Boday, B. Muriithi, R. J. Stover, and D. A. Loy, *J. Non-Cryst. Solids*, 2012, **358**(12), 1575-1580.
8. S. Bhadra and D. Khastgir, *Eur. Polym. J.*, 2007, **43**(10), 4332-4343.
9. H. Gu, J. Guo, X. Zhang, Q. He, Y. Huang, H. A.

*Corresponding author, Tel: +86-15542152720
e-mail address: khalidthebo@yahoo.com

Colorado, N. Haldolaarachchige, H. Xin, D. P. Young, and S. Wei, *J. Phys. Chem. C*, 2013, **117**(12), 6426-6436.

10. H. Xia and Q. Wang, *J. Appl. Polym. Sci.*, 2003, **87**(11), 1811-1817.

11. M. Babazadeh, F. Zalloi, and A. Olad, *Synthesis and Reactivity in Inorganic, Metal-Organic, and Nano-Metal Chemistry*, 2015, **45**(1), 86-91.

12. Z. Hu, L. Zu, Y. Jiang, H. Lian, Y. Liu, X. Wang, and X. Cui, *Polymer Composites*, 2015.

13. A. Riede, M. Helmstedt, V. Riede, J. Zemek, and J. Stejskal, *Langmuir*, 2000, **16**(15), 6240-6244.

14. C. C. S. Pedroso, V. Junqueira, C. P. L. Rubinger, T. S. Martins, and R. Faez, *Synth. Met.*, 2013, **170**, 11-18.

15. M. Gill, J. Mykytiuk, S. P. Armes, J. L. Edwards, T. Yeates, P. J. Moreland, and C. Mollett, *J. Chem. Soc., Chem. Commun.*, 1992(2), 108-109.

16. M. Gill, F. Baines, and S. Armes, *Synth. Met.*, 1993, **55**(2), 1029-1033.

17. H. Nur, N. A. Rahman, S. Endud, and L. K. Wei, *Malaysian Polymer Journal*, 2007, **2**(2), 12-21.

18. S. Armes, S. Gottesfeld, J. Beery, F. Garzon, and S. Agnew, *Polymer*, 1991, **32**(13), 2325-2330.

19. S. Jang, M. Han, and S. Im, *Synth. Met.*, 2000, **110**(1), 17-23.

20. M. Kim, S. Cho, J. Song, S. Son, and J. Jang, *ACS Appl. Mater. Interfaces*, 2012, **4**(9), 4603-4609.

21. H. Yilmaz, H. Zengin, and H. I. Unal, *J. Mater. Sci.*, 2012, **47**(13), 5276-5286.

22. H. Zengin and B. Erkan, *Poly. Adv. Technol.*, 2010, **21**(3), 216-223.

23. F. Kanwal, S. A. Siddiqi, S. Tasleem, G. Sakina, and T. Jamil, *J.Chem.Soc.Pak.*, 2009, **31**(6), 882-887.

24. S. Wang, L. Sun, Z. Tan, F. Xu, and Y. Li, *J. Therm. Anal. Calorim.*, 2007, **89**(2), 609-612.

25. J. Yang, X. Wang, X. Wang, R. Jia, and J. Huang, *J. Phys. Chem. Solids* 2010, **71**(4), 448-452.

26. J. Hlavay, K. Jonas, S. Elek, and J. Inczedy, *Clays Clay Miner.*, 1978, **26**(2), 139-143.

27. S. Wang, L. Sun, Z. Tan, F. Xu, and Y. Li, *Journal of thermal analysis and calorimetry*, 2006, **89**(2), 609-612.

28. J. Yang, X. Wang, X. Wang, R. Jia, and J. Huang, *Journal of Physics and Chemistry of Solids*, 2010, **71**(4), 448-452.

29. X. Li, W. Chen, C. Bian, J. He, N. Xu, and G. Xue, *Appl. Surf. Sci* 2003, **217**(1), 16-22.

30. L. Shao, J. Qiu, M. Liu, H. Feng, G. Zhang, and L. Qin, *Synthetic Metals*, 2010, **160**(1), 143-149.

31. S. Wang, Z. Tan, Y. Li, L. Sun, and T. Zhang, *Thermochimica Acta*, 2006, **441**(2), 191-194.

*Corresponding author, Tel: +86-15542152720
e-mail address: khalidthebo@yahoo.com